ISSN 0027-1349, Moscow University Physics Bulletin, 2014, Vol. 69, No. 4, pp. 275–286. © Allerton Press, Inc., 2014.
Original Russian Text © S.V. Bakurskiy, A.L. Gudkov, N.V. Klenov, A.V. Kuznetsov, M.Yu. Kupriyanov, I.I. Soloviev, 2014, published in Vestnik Moskovskogo Universiteta. Fizika, 2014, No. 4, pp. 3–14.

CONDENSED MATTER PHYSICS

Progress in the Area of New Energy-Efficient Basic Elements for Superconducting Electronics

S. V. Bakurskiy[a], A. L. Gudkov[c], N. V. Klenov[a], A. V. Kuznetsov[a], M. Yu. Kupriyanov[b], and I. I. Soloviev[b]

[a] *Department of Physics, Moscow State University, Moscow, 119991 Russia*
[b] *Skobeltsyn Institute of Nuclear Physics, Moscow State University, Moscow, 119991 Russia*
[c] *Lukin Scientific Research Institute of Physical Problems, Zelenograd, Moscow, 124460 Russia*
e-mail: r3zz@mail.ru, gudkov@niifp.ru, nvklenov@gmail.com, kuznetsov-1992@mail.ru, mkupr@pn.sinp.msu.ru, igor.soloviev@gmail.com

Received February 24, 2014; in final form, March 31, 2014

Abstract—This review is devoted to a discussion of the prospects for solving the problem of a low degree of integration of the traditional elements for promising (due to the high performance and extremely low energy dissipation) superconducting digital electronics. We define three main directions on the path to compact multi-element Josephson electronic systems: (1) reduction of the Josephson junction to submicron size, (2) decrease of the area of standard logic cells, and (3) fabrication of a compact and rapid Josephson memory. We present the physical foundations of Josephson elements in order to show the fundamental constraints on establishing standard submicron tunnel contacts and compact logic cells/memory elements. This survey clearly demonstrates the essence of breakthrough technological solutions to create ultrasmall heterostructures with desired settings, reduce and optimize logic cells, and create memory unit cells based on Josephson junctions with magnetic layers.

Keywords: superconductivity, rapid single-quantum logic, magnetism, Josephson effect, Josephson junction, internal shunt, Josephson memory.

DOI: 10.3103/S0027134914040043

1. INTRODUCTION

Under the contemporary information era, an exponential growth of the amount of data to be processed in-line is characteristic for almost all the domains of science and technology. Against the background of rising costs of material resources, the impetuous increase of the energy consumption by systems for processing and transmission of information turns into a serious problem for the domestic and global economy [1]. Today, computer and telecommunication complexes consume about 5% of the global electric power and this percentage will increase up to 10% in the next 5 years. Let us adduce the following figures: the energy consumption by the 500 best supercomputers was 0.25 GW in 2011, which, in terms of a supercomputer (that performs about 10^{15} operations per second), is an average of 0.5 MW. Moreover, the energy target for only one next-generation supercomputer, i.e., a system of the exaFLOPS class (which performs about 10^{18} operations per second), will be 0.5 GW. For comparison, the power of the BWR-3 reactor of the Fukushima 1 nuclear power plant was only 46 GW.

On the path of using the traditional element base, we see no possibilities for the fundamental solution of this problem. The characteristic level of energy consumption in circuits based on the standard silicon technology is about 5 fJ per logical operation. For exaFLOPS computers, the economically feasible level of energy consumption must be at least by two or three orders of magnitude lower than that for modern semiconducting technologies and be no greater than 20 aJ [2, 3].

Taking into account the impetuous approach of the characteristic dimensions of basic elements for semiconducting electronics to atomic scales (which excludes, for fundamental reasons, the further use of outdated approaches to solving the problem of increasing their performance), a rising tide of interest in alternative principles of creating the electronics becomes sound.

Among possible alternatives, the digital superconducting Josephson technology can be singled out; it possesses a number of advantages in terms of such key parameters as the performance (the characteristic frequency of a basic element for superconducting electronics, viz., the Josephson junction, ranges up to hundreds of gigahertz) and ultra-low power consumption (the energy dissipation for a logical operation is merely 0.1 aJ [4] and signals in superconducting cir-

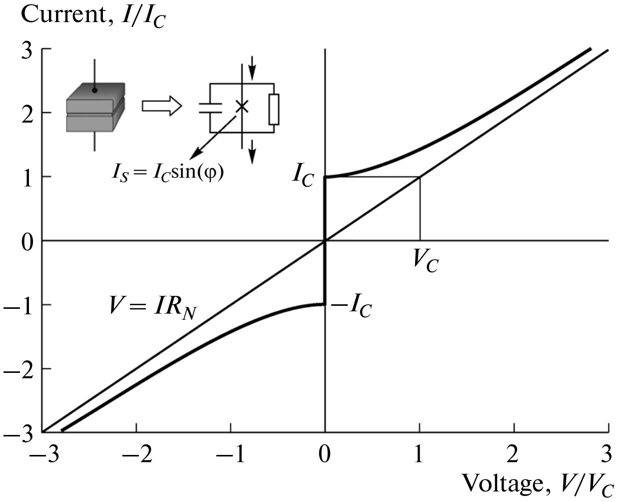

Fig. 1. A typical current-voltage characteristic of a Josephson element within the framework of the resistively shunted junction model with the specification of the critical current, characteristic voltage, and normal resistance. An illustration of the description of the current-transfer mechanism for the resistively shunted junction model is presented.

cuits can be transmitted with little or no loss). Superconducting Josephson circuits created for reversible computing systems are distinguished for their extreme energy efficiency. In such systems, the energy dissipation takes place only when recording and reading information and logical operations are implemented using adiabatic processes, i.e., are performed with little or no energy loss. Experimental studies and theoretical estimates show that the energy efficiency of digital superconducting Josephson circuits is greater by at least four orders of magnitude than that of semiconducting analogues [5] and the energy efficiency of reversible systems based on Josephson circuits has been proven by six orders of magnitude greater and can reach and even overcome the Shannon–von Neumann–Landauer thermodynamic limit for energies of binary transformation [6, 7].

For many years, the wide use of this promising technology has been hindered by high costs of creating and maintaining cryosystems. In recent years, this problem has almost been solved. In particular, rather miniature and cost-effective cooling installations have been developed that provide a stable temperature and are necessary for the superconducting electronics to work [8–10].

Today, one key constraint is a low degree of integration of the on-chip active element, which hinders the creation of fully-superconducting digital systems. This paper is devoted to the review of the progress in the area of optimizing a basic element for the digital superconducting technology, viz., the Josephson junction, to solve this problem.

2. OPERATION PRINCIPLES OF THE JOSEPHSON JUNCTION

From the outset, note that the basic element for superconducting electronics, viz., the Josephson junction, differs in its electrophysical properties from basic elements of the traditional silicon technology (diode and transistor). A Josephson junction is a bipolar device consisting of two superconducting electrodes that are separated by a region in which the superconductivity (modulus of the wave function of electrons in a superconducting state) is considerably quenched. Superconductivity quenching can be provided by geometric factors (for example, narrowing) or by using a thin nonsuperconducting interlayer between the electrodes. Historically, the method for fabricating a Josephson junction, which is based on using a nonsuperconducting interlayer, has proven to be the most compact and practically feasible. The current flowing through such a Josephson junction consists of the following three components: (1) dissipation-free current (this component can be provided, for example, by the induced superconductivity in the nonsuperconducting interlayer, i.e., proximity effect, or by the tunneling of correlated electrons in superconducting state); (2) resistive component of the current; and (3) capacitive component that arises from the overlap of the superconducting electrodes (see Fig. 1).

Due to the quantum nature of the superconducting effect, the electrophysical characteristics of the Josephson junction are considerably determined by the laws of quantum mechanics. Electrons in a superconducting state are described by the complex order parameter $\Delta e^{i\theta}$, so that the phase jump of the order parameter in the weak-coupling region will correspond to the inclusion of the Josephson junction into a closed superconducting circuit. Within the framework of a simple resistively shunted junction model, the current flowing through the Josephson junction is related to the phase jump, which is called the Josephson phase $\varphi = \delta\theta$, with the following relationship [11, 12]:

$$I = I_C \sin\varphi \frac{\hbar}{+2e_0 R_N}\frac{\partial\varphi}{\partial t} + \frac{\hbar C}{2e_0}\frac{d^2\varphi}{dt^2}, \qquad (1)$$

where I_C is the critical current (maximum dissipation-free current to flow through the junction); R_N is the normal resistance of the junction; C if the capacity of the junction; $h = h/2\pi$, h is the Plank constant; e_0 is the electron charge; and t is the time. The form of the dissipation-free current component $I_C\sin\varphi$ reflects the electrical neutrality of the system as a whole and 2π-periodicity of the phase of the order parameter (stationary Josephson effect). The voltage on the Josephson junction is proportional to the derivative of the Josephson phase with respect to time $V = (\hbar/2e_0)\varphi_t$ (nonstationary Josephson effect), which affects the form of the second (V/R) and third (CV_t) terms in

Eq. (1). It is useful to note: Eq. (1) actually corresponds to the equation of motion of a physical pendulum with eigenfrequency $(2e_0I_C/\hbar C)^{1/2}$ with the Josephson phase φ corresponding to the angle of the pendulum's deviation from a stable equilibrium position.

For the voltage on the Josephson junction to occur, the total current (which, in terms of mechanics, induces the torque moment) is required to be greater than the critical current $I > I_C$. The capacity that ensures the storage of electrical energy, which is proportional to the squared rate of change of the Josephson phase, determines the inertial behavior of the system, which make itself evident in the fact that the current of returning into the superconducting state for the Josephson junction may be smaller than the critical current $I_r < I_C$. With the definiteness of the state of the Josephson element being required for digital circuits to operate correctly, the effect of the capacitive component of the current is reduced by adding an external or internal shunt; this is similar to increasing the "viscosity" of the system, which is proportional to the weight of the second term in the right part of Eq. (1). In the limit of small capacity, the characteristic frequency of the processes taking place in the Josephson junction [11, 12]

$$\omega_C = \frac{2e_0}{\hbar}I_CR, \tag{2}$$

is proportional to the product of the critical current by the effective normal resistance R ($R^{-1} = R_N^{-1} + R_S^{-1}$, where R_S is the resistance of the shunt). Values of the critical current and normal resistance are determined by the geometric dimensions of the junction structure, transparency of boundaries of its interfaces, and electrical properties of the interlayer material.

3. PROBLEM OF CREATING A COMPACT JOSEPHSON ELEMENT

Today, the most proven technology for fabricating Josephson junctions is based on forming the superconductor–insulator–superconductor (SIS) layers Nb/AlOx/Nb with tunnel-type charge transport. The traditional semiconducting methods [13], including sputtering, etching, and planarization, are used to form the junction structure. Unfortunately, such a method of fabrication is not suitable for creating submicron Josephson elements. In order to ensure the required accuracy of information processing in digital superconducting devices (whose operation principles are described below), the critical current I_C must be at least by two orders of magnitude greater then the effective noise current [14], which amounts to $I_f \approx 0.18$ μA for helium temperatures ($T = 4.2$ K). This means that the value of the critical current must be $I_C \geq 100$ μA, which, for the implementable critical-current densities $J_C \leq 10$ kA/cm^2, is in agreement with the size of the Josephson junction $S \geq 1$ μm^2. It is seen that for the area of junction $S = 0.1 \times 0.1$ μm^2, the density of the critical current $J_C = I_C/S$ must exceed 1000 kA/cm^2. For the traditional technology of creating tunnel junctions [15, 16], such current densities are not feasible, since, beginning with values that are already smaller by an order of magnitude, the increase of J_C is accompanied by a considerable increase in the spread of the critical current of junctions within a chip. This spread is related to the decrease in the thickness of the insulator interlayer up to several units of atomic-lattice spacing, which is comparable with layer inhomogeneities and uncontrolled deviations of planar dimensions of the structure from specified values. Moreover, as is shown above, it is required to shunt the effect of capacity (which proves to be considerable in the case of the tunnel structure) for the Josephson junction to operate correctly. A proven solution is the use of external resistors that are connected parallel to the junction. In actual practice, such a technological solution results in an extra increase of the junction size by 10–20 μm^2 [13].

Josephson junctions with an internal shunt, from which the superconductor–normal metal–superconductor (SNS) junction seems to be the simplest one, are free from the above disadvantages. In SNS structures, the required current densities are easily reachable and the effect of capacity is small to negligible. At the same time, the high characteristic frequency (2) of the Josephson junction, which is determined by the product of the critical current by the normal resistance, is difficult to ensure. In truth, in order to ensure high densities of the critical current, the material of the normal interlayer must possess a high effective coherence length (the distance on which the modulus of an "induced" order parameter for electrons in superconducting state is reduced in the normal metal by e times) that is

$$\xi_{NC}^{*} = \frac{\hbar v_F}{2\pi k T_C}, \tag{3}$$

provided that the free path of electrons in the metal ℓ is considerably smaller than ξ_{NC}^{*} and other characteristic spatial scales of the problem (clean limit) or

$$\xi_{ND}^{*} = \sqrt{\frac{\hbar D}{2\pi k T_C}}, \tag{4}$$

in the opposite case (the dirty limit). Here, v_F and $D = v_F\ell/3$ are the electron velocity on the Fermi surface and the diffusion coefficient for the normal metal, respectively; k is the Boltzmann constant; and T_C is the critical temperature for superconducting order parameter. As is seen, the coherence length is increased with increasing electron velocity on the

Fermi surface, i.e., increasing conductivity of the material.

On the other hand, when niobium, which possesses a high specific resistance in a normal state, is used as a superconductor in the standard superconducting technology, the use of a good conductor (Au, Cu, or Al) as the normal interlayer of the Josephson junction results in a considerable degradation of superconductivity in the vicinity of the superconductor–normal metal (S–N) interface. In fact, the quenching of superconductivity via the proximity effect determines the parameter

$$\gamma = \frac{\rho_S \xi^*_{SD}}{\rho_N \xi^*_{ND}}, \tag{5}$$

where $\rho_{S,\,N}$ and $\xi^*_{SD,\,ND}$ are the normal specific resistances and coherence lengths of the contacting superconductive and normal materials. The parameter (5) is proportional to the ratio between the number of the normal electrons that are able to diffuse from N into S in a unit time and the number of the correlated electrons transporting the dissipation-free current that are able to diffuse in the opposite direction in the same time. It is qualitatively clear that, even for comparable coherence lengths $\xi^*_{SD} \sim \xi^*_{ND}$ in the case of a great value of γ, which is determined by the ratio ρ_S/ρ_N, the excess of normal electrons will take place in a superconducting part of the S–N interface, resulting in an almost complete quenching of superconductivity in the vicinity of the S–N interface.

The limit of small γ corresponds to the so-called severe boundary conditions: there, almost no superconductivity quenching in the S electrode and the normal metal in the SNS structure is able to transfer a noticeable dissipation-free current. In order to implement the boundary conditions, a normal metal must possess a specific resistance that is considerably greater than that of niobium and the thickness of the metal (for example, palladium–gold alloy or titan) must not exceed its coherence length, which amounts to nanometers for such conductors and is comparable with the roughness of the boundaries in a heterostructure [14]. Thus, for actual SNS Josephson junctions, the normal resistance proves to be extremely low: from several milliohms (Nb–Ti–Nb) to tens of milliohms (Nb–PdAu–Nb); while the characteristic voltage $I_C R_N$ is from tens (Nb–Ti–Nb) to hundreds (Nb–PdAu–Nb) of microvolts [17, 18], which corresponds to the characteristic frequency of the junctions ($\omega_c/2\pi$ = 5–50 GHz), which is considerably lower than the corresponding frequency of tunnel Josephson junctions; this lies in the range of hundreds of gigahertz.

A more promising approach to miniaturizing the basic element of superconducting digital circuits is the use of Nb–αSi–Nb Josephson heterostructures. The interest in amorphous silicon (αSi) as a weak-coupling material has been due to its lower potential barrier as compared to aluminum oxide. It seemed that this should open the possibility of producing tunnel structures with thicker and more workable barriers. Experimental studies has shown that either a relatively poor insulator whose transport properties are largely determined by the tunneling of quasi-particles ("uncorrelated" electrons in normal state) through localized states or a material with a metallic nature of conductivity result from successive depositions depending on the character and degree of doping of silicon with niobium.

In the first case, tunneling is the main mechanism of providing the transport of a charge through the weak-link region. Thus, the conducting channels arise by means of elastic and inelastic resonant tunneling. An inelastic channel cannot ensure the transport of the superconducting (dissipation-free) current and, in fact, determines the value of the normal resistance that shunts the junction. In contrast, the elastic channels are similar to the superconducting jumpers in a matrix with tunneling conductance.

In the second case (a material with a metallic nature of conductivity), amorphous silicon is doped with Nb atoms via diffusion up to the complete degeneracy of a semiconductor, i.e., until the interlayer αSi is turned into a high-resistance metal. In this case, $\rho_N \gg \rho_S$ and the superconductivity quenching in Nb electrodes is small to negligible. The values of the normal resistance and characteristic voltage, which are obtained on the Josephson junctions of the butt and planar types (in some works, tungsten doping is used) [19–22], are rather great: up to 0.06 Ohm and up to 0.3 mV, respectively. Due to the inelastic tunneling of electrons through states localized on admixtures in αSi, the internal shunt ensures the definite voltage-current characteristic and small inertia for the compact Nb–αSi–Nb Josephson elements (in size up to $2.5 \times 2.5\ \mu m^2$). It is significant that the thickness of the isolation barriers based on aluminum oxide in SINIS junctions (at such structures, rather high normal resistances and characteristic voltages have been sought) is about ten times smaller than the thickness of the weak-coupling region for the heterostructure Nb–αSi–Nb with comparable densities of critical current. Therefore, the use of Josephson junctions with doped silicon requires no work with ultrathin layers (~1 nm in thickness) with irreproducible characteristics. All the above features of the Josephson elements with amorphous silicon in the weak-coupling region offer the prospect of their advantageous use in superconducting devices (correct operation of the digital circuits with characteristic frequency up to 165 GHz has been reported [23]). We do not see fundamental obstacles to creating submicron Josephson junctions in Nb–αSi–Nb: densities of critical currents above 100 kA/cm^2 have been experimentally modeled [20]. The successful creation of Josephson stacks with an internal shunt [24] opens the way to using the third dimension for an extra enhancement of the degree of integration for superconducting integrated circuits.

4. INFORMATION REPRESENTATION IN SUPERCONDUCTING DIGITAL CIRCUITS AND RESTRICTIONS ON THE DEGREE OF INTEGRATION

A fundamental property of the superconducting state of a material is the expulsion of the external magnetic field (up to the value of the critical current that destroys the superconductivity). At the same time, in the superconductor-free region within the superconducting loop, the magnetic flux is free to exist in a stable state, but its value will be quantized, i.e., will be a multiple of the minimum possible magnetic flux $\Phi_0 = h/2e_0$, which is called a magnetic flux quantum. From the physical viewpoint, the phenomenon of magnetic flux quantization reflects the momentum conservation law (taking into account the momentum created by the magnetic flux) and 2π-periodicity of the phase of a superconducting order parameter (similarly to the Bohr–Sommerfeld quantization rule).

The principle of processing and storing information in superconducting digital electronics (which is the most widespread today) was proposed in the late 1980s by K.K. Likharev, V.K. Semenov, and O.A. Mukhanov from Moscow State University [25–27]. An information bit is represented here in the form of the presence or absence of a magnetic flux quantum in the simplest superconducting loop (quantum interferometer), which involves Josephson junctions (see Fig. 2a) The total magnetic flux in such a loop, which corresponds to the total phase jump at Josephson junctions and phase gradient on inductances of bonding superconductors, will be a multiple of the magnetic flux quantum so that the phase incursion of the superconducting order parameter with respect to the loop will be a multiple of 2π.

A mechanical analogue of the closed superconducting loop is a spring fixed at both ends. The application of an external magnetic field corresponds to twisting the spring with a corresponding increase of energy storage. The inclusion of two Josephson junctions into the closed loop is similar to the replacement of severe boundary conditions by softer ones whereby the spring is fixed to two pendulums along the axis of their fastening. The deviation of one pendulum from equilibrium results not only in the twisting of the spring but also in the deviation of another pendulum from equilibrium according to the end moment of its inertia and the stiffness of the spring. Thus, only some of the energy will pass into the energy stored in the spring. It is obvious that for a low spring stiffness (a great inductance of bonding superconductors), the pendulums (Josephson junctions) are weakly coupled. In this case, the position when one pendulum is

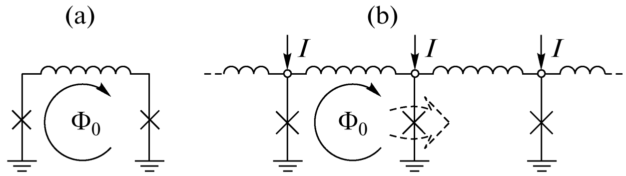

Fig. 2. (a) An example of a superconducting loop that involves two Josephson junctions (shown by cross hairs): the total magnetic flux in the loop is a multiple of the flux quantum Φ_0 and the circular arrow shows the circulating current that corresponds to the magnetic flux in the loop. (b) Josephson transmitting line: the magnetic flux quantum is transferred between the loops due to the Lorentz force created by the applied current I.

deflected through the angle that exceeds the angle of unstable equilibrium π and another pendulum through an angle less than π (the state that corresponds to the presence of the magnetic flux in a loop with Josephson junctions) will be stable. By increasing the number of parallel-coupled Josephson junctions (the number of pendulums in the chain) and applying the bias current (torque moment) as shown in Fig. 2b, the magnetic flux can be transferred from one loop to another along the chain due to the Lorentz force (wavepacket propagation in a discrete chain of pendulums). Such a chain is called a Josephson transmitting line and the above process corresponds to the transmission of information in circuits of superconducting digital electronics.

In digital Josephson circuits based on the combination of quantum interferometers with Josephson transmitting lines, the pulse clock principle of operation is applied. Magnetic flux quantums and rapid single-quantum voltage pulses related to their motion (RSFQ pulses for which $\int V dt = \Phi_0$) are used as clock pulses, i.e., they divide the operating time into clock periods. A magnetic flux quantum that appears at the input or output of the system during a clock period is regarded as the logical 1, while the absence of a quantum is the logical 0; for gate circuits, the clock frequency can reach 770 GHz [28].

Note that the degradation of coupling inductance of a transmitting line (the increase of spring stiffness) will correspond to the reduction of discreteness of a chain, resulting in the distribution of the magnetic flux onto several loops; therefore, the value of inductance is chosen so that a flux quantum is dominantly localized in one loop. Being formulated in the form of an inequality $I_C L/\Phi_0 > 1$, this requirement, which takes the actual densities of the critical current for Josephson junctions $j_C \approx 1$ kA/cm^2 into account, leads to the characteristic value of geometric inductance for the loop: $L \geq 10$ pH. From this condition the restriction follows on the minimum dimensions of elementary circuits for superconducting electronics. In the case of actual circuits, the continuous shield superconducting layers, which protect circuits against external magnetism, lie parallel to functional layers from the top and bottom. These layers are responsible for the concentration of magnetic field in the vicinity of junctions and effectively decrease their inductance, which, in turn, leads to the necessity for an extra increase in the dimensions and a decrease in the degree of the integration of circuits.

The actual size of an elementary loop consisting of two parallel-coupled Josephson junctions is $S_{\text{cell}} \geq 200\ \mu\text{m}^2$. This provides an estimate of the maximum degree on integration in terms of the number of Josephson junctions on a chip; for example, N = 1.25×10^5 junctions for a chip size of $5 \times 5\ \text{mm}^2$. In actual practice, the degree of integration proves to be an order of magnitude lower, so actual circuits involve approximately $1{-}1.5 \times 10^4$ junctions. For example, an 8-bit arithmetic logic unit, whose operation on the frequency of 20 GHz has recently been demonstrated [29], involves only $N = 7710$ junctions.

The low degree of integration also hinders the fabrication of a superconducting memory with sufficient capacity. The record capacity of the superconducting random access memory is only 4 Kb [30]. Hybrid superconducting–semiconducting memory is used today as a way out of this situation [31, 32]. The operation of a hybrid random-access device with a capacity of 64 Kb has been experimentally demonstrated [31]. Unfortunately, the use of the hydride approach, which assumes the transfer of data between chips with superconducting logic circuits and semiconducting memory, markedly impairs the performance and increases the total energy consumption of systems.

5. JOSEPHSON π-JUNCTIONS

From the above discussion it follows that the primary cause of the low degree of integration of superconducting digital circuits is the necessity for storing and transferring the magnetic flux quantum Φ_0, which imposes a restriction on the value of the geometric inductance of an elementary loop with Josephson junctions. The solution of this problem may lie in the use of the so-called Josephson π-junction. The Josephson phase of such a junction in the equilibrium state is shifted by π, which determines the change in the form of the dissipation-free component in Eq. (1) and is formally similar to changing the sign before it:

$$I = I_C^{\pi}\sin(\varphi + \pi) = -I_C^{\pi}\sin(\varphi). \qquad (6)$$

In the case where the critical current of the π-junction (Josephson element with current–phase ratio (6)) considerably exceeds the critical currents of other junctions, it will act like nonlinear inductance $L_J = \Phi_0/(2\pi I_C^{\pi}\cos(\varphi))$ and ensure an extra decrease in the phase of a superconducting order parameter by π.

In a number of works [35–37], the possibility of the complete replacement of the geometric inductance of a logical element loop with a π-junction while preserving the range of parameters of a stable system operation has been experimentally demonstrated. Using π-junctions, the dimension of the superconducting memory, whose elementary cell is a loop with one or two Josephson junctions [27], can also be reduced considerably. The possibility of providing the negligible geometric inductance considerably enhances the compactness of circuits and, taking the above possibility of stacking Josephson junctions into account, opens a real prospect for scaling the element base of superconducting electronics into the submicron domain [35]. At the same time, for certain circuits (for example, the Josephson transmitting line discussed above), the phase shift by π provides no extra advantages [36]; therefore, standard junctions with a greater value of the critical current (or a stack of several junctions) can be used to reduce their geometric inductance. Notwithstanding the fact that the π-junction always remains in a superconducting state in the proposed modifications of circuits, its normal resistance R_N and Josephson inductance L_J form a low-frequency filter with the characteristic time constant $\tau_\pi = |L_J|/R_N = \Phi_0/|(2\pi I_C^{\pi}\cos(\varphi))|$. The performance of a circuit is not reduced by including a π-junction into it provided that the product $I_C R_N$ of the π-junction is on the order of the corresponding magnitude for standard Josephson junctions. The experimental implementation of π-junctions with required settings has long been problematic. In recent years, technological solutions have been found with the participation of scientists from Moscow State University that provide the implementation of π- and even φ-junctions (junctions with an arbitrary phase shift in an equilibrium state φ_*, $0 < \varphi_* < \pi$) by including magnetic layers into the weak-link region [39–41]. The following section describes the physical principles underlying these technological solutions in detail.

6. PRINCIPLES OF MAGNETIC JOSEPHSON JUNCTIONS FABRICATION

We recall that the dissipation-free current (supercurrent) is usually transferred by the so-called singlet Copper pair: pairs of correlated electrons with converse projections of spins onto the quantization axis [42, 43]. Therefore, superconductivity is broken up under the action of even a relatively weak magnetic field, which tends to align all the spin magnetic moments of electrons in one direction.

Particularly, in a ferromagnetic (F), both heat energy and exchange magnetic field (with energy H) contribute to the destruction of Copper pairs. The coherence length for an F-material in the dirty limit, as follows from expression (4), describes the similar value for an N-material) [44]:

$$\xi_{F1,2} = \left(\frac{\hbar D}{((k_B T)^2 + H^2)^{\frac{1}{2}} \pm k_B T} \right)^{\frac{1}{2}}. \quad (7)$$

Here, ξ_{F1} and ξ_{F2} are the real and imaginary parts of the complex coherence length for the ferromagnetic, respectively. The real part given by expression (7) determines the rate of the exponential attenuation of the amplitude of the probability density to reveal interelectronic Copper correlations, while the imaginary part specifies the period of sign-variable oscillations of the function. The specific behavior of the superconducting correlations in the vicinity of the SF interface and the comparison with the case of the SN interface are shown in Fig. 3. One of manifestations of this specificity of the superconductor/ferromagnetic hybrid structures is the sign-variable oscillation of the critical current of a Josephson SFS junction, which provides the basis for the implementation of magnetic π-junctions [45].

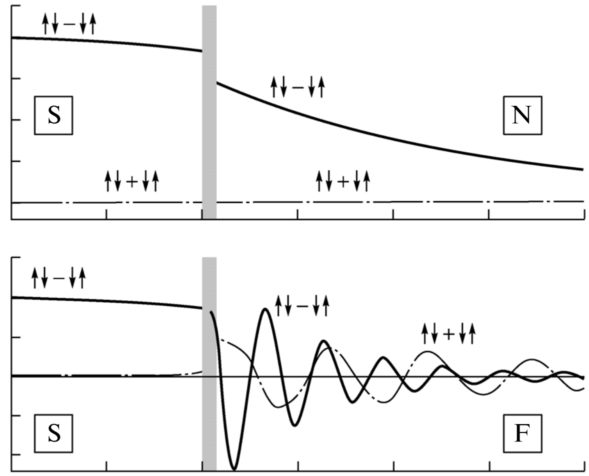

Fig. 3. The behavior of the functions that determine the amplitudes of the probability of finding singlet and triplet superconducting electron correlations in the vicinity of SN (from top) and SF (from bottom) interfaces.

Attempts to create compact magnetic superconducting memory elements, in which information storage is not related to the presence or absence of a flux quantum in the circuit but is provided by different orientations of the stable magnetization of a ferromagnetic layer, occur as a natural development of works on creating magnetic Josephson junctions. For a long time, the antagonism between superconductivity and ferromagnetism hindered the creation of compact magnetic superconducting memory elements controlled by weak magnetic and current signals that are typical for superconducting devices. Historically, the memory system [46, 47] that was first implemented involved direct contact between the superconductor (or the weak-link region of a Josephson junction with induced superconductivity) and the simplest magnetic valve. A structure involving two layers of F-materials with different coercive forces, which were separated by a nonferromagnetic interlayer [48], was used as the control valve, which ensured the control of mutual orientations of the F-layer magnetization due to external fields. Obviously, Cooper pairs in the neighborhood of the region of contact with the valve will deteriorate; in the case of a parallel (ferromagnetic) orientation of magnetizations in the layers, the density of the critical current of the superconductor (the Josephson junction) will be suppressed to a much greater extent than in the case of an antiparallel (antiferromagnetic) orientation. In order to implement the valve, greater values of magnetic moments must be ensured in F-films for the magnetic field created by the films to change considerably the superconducting properties of the structure. Hence, greater magnetic fields of remagnetization (near 20–40 mT) were to be created to control the flowing current. At a later time, direct contact between the superconducting circuits and the magnetic material was ruled out: the ferromagnetic point, whose magnetization is controlled via a separate conducting line that affects the neighboring Josephson junction exactly due to the magnetic field created by it [49].

A magnetic Josephson junction that involves magnetic multilayer structures in the immediate region of weak link proves to be an indubitably more compact element [39–41, 50, 51]. The simplest solution is the use of the magnetic valve described above as weak link [48]. In particular, the change from ferromagnetic to antiferromagnetic magnetization orientation of F-layers in the tunnel SFIFS junctions has been shown to result in the amplification of the critical current, as well as the change of its sign (transition to the π-state) [52, 53].

At one time, reducing the value of the magnetic fields required one to control the critical current of the Josephson junction, it has been proposed to use ferromagnetic materials with low coercive force: the possibility of switching between two states with considerably different values of critical current by means of weak magnetic fields (~1 Gs) has been demonstrated for the superconductor–ferromagnetic–superconductor (SFS) structure using a $Pd_{0.99}Fe_{0.01}$ layer (the Curie temperature is just ~15 K) in the region of weak link [54]. We emphasize that only one magnetic layer, whose two stable states are the "magnetized" and "demagnetized" states, is used in such a structure (with cluster-type magnetism [55]): different values of the effective exchange field in an F-layer lead to different degrees of the induced-superconductivity quenching in the weak-link region and different values of the critical current of a Josephson junction. A conceptual sketch of a relatively compact Josephson memory ele-

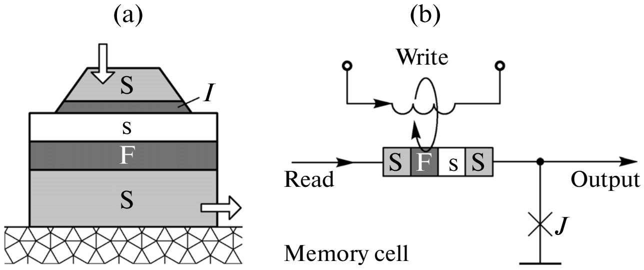

Fig. 4. (a) A conceptual sketch of the SIsFS structure and (b) a conceptual sketch of the memory cell based on the SIsFS structure.

ment whose operating principle is based on the switching between two states with different critical currents is shown in Fig. 4b: in a stable state with a high critical current a magnetic Josephson junction, when passing a one-quantum momentum, is not turned into a resistive state and does not hinder the wave propagation along the transmitting line; in the opposite case, the element is turned into a resistive state and "releases" a flux quantum from the transmitting line. As is seen, the size of the memory element itself is same as the size of the junction in this case.

7. MAGNETIC JOSEPHSON JUNCTIONS WITH INTERMEDIATE SUPERCONDUCTING LAYERS IN THE REGION OF WEAK LINK

The integration of the Josephson memory based on magnetic Josephson junctions with the circuits of rapid superconducting digital electronics will be successful provided that the structures under study meet the two following requirements:

* Rapid remagnetization of a ferromagnetic layer using a small magnetic field for the "Write" operation;

* Short switching time of a Josephson junction (the value I_CR_N of a magnetic junction must be on the order of the corresponding value of a standard junction) for the "Read" operation.

The insulating interlayer increases the resistance of a Josephson junction R_N; however, the benefit is that the critical current I_C is decreased and, as is seen from expression (2), the characteristic frequency $\sim I_CR_N$ remains relatively low (1–2 GHz). Low characteristic frequencies considerably limit the use of patented SIFS structures both as π-junctions and as the element base for the rapid Josephson memory. There are attempts to considerably increase the critical current due to creating triplet superconducting correlations for which the spin part of the wave function has the form of $|\uparrow\uparrow\rangle$ or $|\downarrow\downarrow\rangle$, on special magneto-active regions: the attenuation length of such correlations in a ferromagnetic is rather high [56–59]. However, this problem can successfully be solved by introducing an extra superconducting layer into the weak-link region (see Fig. 4a). The theoretical and experimental studies carried out with the participation of the scientists from Moscow State University demonstrate the possibility of creating the basic Josephson element with controlled critical current, whose characteristic frequency differs from that of the standard tunneling SIS junction by less than 25% [60, 61]. Referring to Fig. 5a, which generalizes the results of applying the algorithm for the self-consistent analysis of current transport for one-dimensional Josephson structures that involve a multicomponent interlayer of a ferromagnetic and/or an insulator (the algorithm was developed at Moscow State University), the structure with an extra superconducting layer in the weak-coupling region has the maximum possible absolute value of the product I_CR_N. Moreover, in the area of interest on the parameter plane, the absolute value of the product I_CR_N varies slightly for small changes of the effective exchange field (see Fig, 5b). This provides the experimental creation of Josephson junctions with small parameter degradation (such parameters of an individual junction remain unchanged even after a great number of write/rewrite cycles), which is mandatory for any applications in practice [62, 63]. A small change in the magnetization of the interlayer in the external magnetic field allows the critical current I_C of a Josephson junction to be efficiently controlled. Two states of the junction with minimum and maximum I_C can be used to store the logical zero and logical unit, with both states being stable in time.

Owing to the combination of the superconductor and weak ferromagnetic, the magnetic Josephson SIsFS junctions provide, with the optimal choice of the effective thickness of the ferromagnetic interlayer, the shift of phase of the dissipation-free current component by π, which allows a π-junction with great I_CR_N to be implemented.

Finally, for certain thicknesses of the F-layer, an abrupt thermal 0-π transition [61] is feasible, which allows a 0-π switch based on the S–IsF–S element to be constructed. Let us clarify the design of the switch proposed by the scientists from the Moscow State University [64]. Such an element implemented in a planar geometry consists of the two superconducting electrodes and a weak-link region that involves the magnetic layer with direct or resonant conductivity, the insulating layer or superconducting layer between them, and two auxiliary superconducting leads for setting the current through the magnetic layer. The difference from well-known Josephson SFS structures is the fact that when the current flows in the magnetic layer localized in the weak-link region between the superconducting electrodes, energy liberation takes place, leading to an increase in the effective working temperature of the junction that is accompanied by a sudden change of the value and sign of the critical current (see Fig. 6). The dashed line shows the tempera-

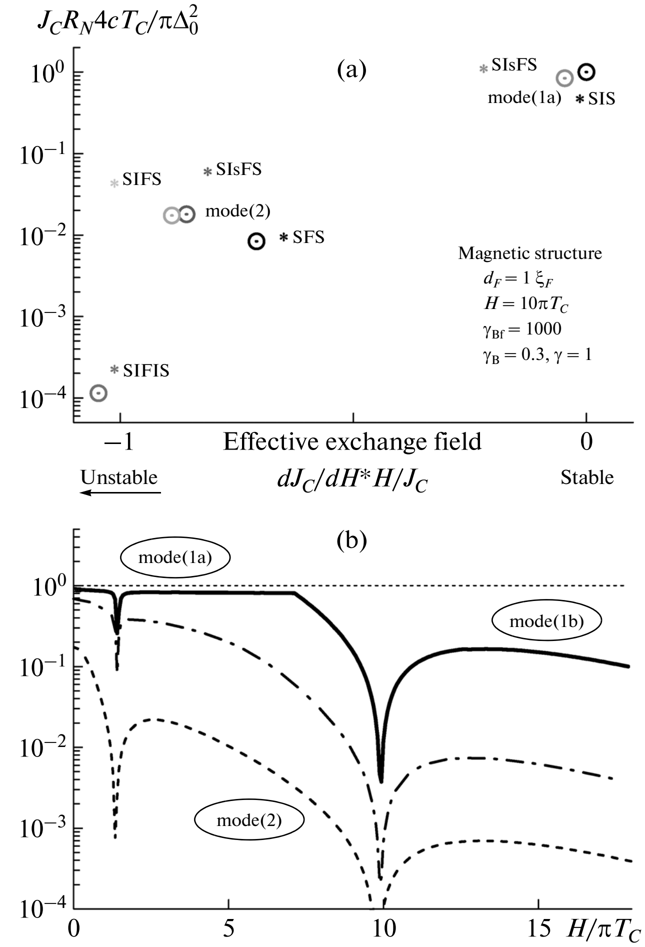

Fig. 5. (a) The absolute value of the normalized product $I_C R_N$ of the SIsFS structure and the stability of this parameter when changing the effective exchange field in an F-layer for two significant limit cases: (mode 1a) the order parameter on the island S' is different from zero and (mode 2) the superconductivity in this interlayer is completely quenched. For comparison, similar design values are presented for the structures of superconductor–insulator–superconductor (SIS), superconductor–ferromagnetic–superconductor (SFS), superconductor–insulator–ferromagnetic–superconductor (SIFS), etc. (b) Dependence of the normalized product $I_C R_N$ of the SIsFS structure on the effective exchange energy controlled by the applied magnetic field for the above cases [61]. For both the figures, J_C is the critical current density, R_N is the resistance of the junction in a normal state, T_C is the critical temperature of the used superconductor, and Δ_0 is the "coupling amplitude" that determines the concentration of superconducting correlations away from the boundary of the S-material.

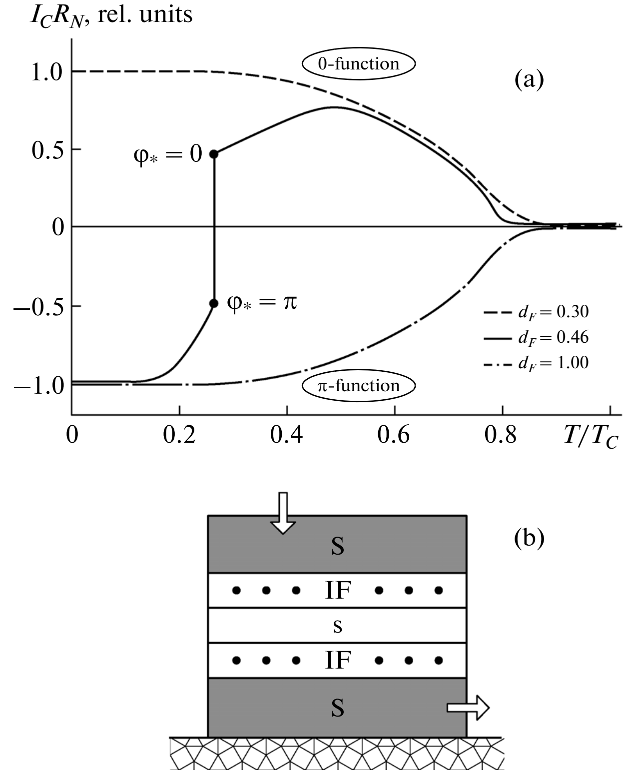

Fig. 6. (a) The dependencies of the normalized critical current of the SIsFS structure on temperature normalized with respect to the critical temperature of the superconducting materials and (b) a conceptual sketch of the SIFsFIS structure.

ture dependence of the normalized critical current for the case where the thickness of the magnetic layer is sufficiently small (in superconducting materials, the ratio of the thickness to the coherence length is 0.3 and lower): the critical current is positive for any temperature, the case of the so-called zero state occurs; the product of the critical current by the normal resistance is sufficiently great and is close to values typical for SIS structures. The dotted line shows the case when the thickness of the magnetic layer is sufficiently small (in superconducting materials, the ratio of the thickness to the coherence length is 1 and greater): the critical current is negative for any temperature, the case of the so-called π-state occurs; the product of the critical-current absolute value by the normal resistance is sufficiently great and is close to values that are typical for SIS structures. The solid line shows the normalized dependence of $I_C(T)$ for the case when the thickness of the magnetic layer provides efficient switching between states with positive and negative values of I_C. When the ratio of the "magnetic" thickness to the coherence length in superconducting materials is 0.46, the critical current abruptly changes its value and even sign when changing the normalized temperature by 0.2 (see Fig. 6a). It is this fact that allows the controlled 0-π switch, which might be useful in many different applications, to be implemented based on such a structure [37, 65, 66].

Note that a number of significant drawbacks are peculiar to the SIsFS structure as a memory element. As in the case of SIS junctions, SIsFS elements possess a high capacity and require an external shunt. The use of a metallic ferromagnetic layer results in a strong quenching of superconductivity in electrodes, while the formation of a complex composite interlayer with precision-thin layers (nanolayers) requires two different technologies for I- and F-layers. Moreover, a significant drawback in using any Josephson structures with one magnetic layer as a base for a memory element is the complexity of implementing a reliable half-selective mechanism (operations on an element are performed only in case of the simultaneous injection of two control signals).

We believe that the Josephson junction (implemented in the planar, butt, or bridge geometry) is a more universal and scalable design, whose weak coupling involves two magnetic layers with resonant conductivity and a superconducting layer between them (see Fig. 6b) [67]. When changing the orientation of magnetization of an F-layer in the superconducting film, *s*, which is localized in the region of weak coupling between the magnetic layers, a considerable restoration (quenching) of superconductivity takes place. With the optimal settings, one can provide the phase transition of the intermediate *s*-layer from the normal state to superconducting one or from the superconducting state to normal one. In particular, the transition of the *s*-layer into the normal state means that, instead of two series-connected Josephson junctions (SIFs and sFIS) with relatively large critical currents, we obtain one junction with a complex-IFNFI-region of weak link and a very small critical current. Such a design will allow the half-selective mechanism in the memory matrix to be implemented in a similar way as in the technology for magneto-resistive memory based on magnetic tunnel junctions [68]. In order to provide the compactness of the proposed magnetic junction, amorphous silicon doped with Fe and Ni atoms, which is described in Section 1, should be chosen as the material for magnetic layers with resonant conductivity. With such a "ferromagnetic" doping, the "magnetic layers" are formed in the weak-coupling region, whose mutual magnetization orientations can be controlled using weak external fields. The use of the previously-developed Nb/αSi/Nb (SDS type) Josephson junctions with an internal shunt as a basis will ensure the definiteness of the current-voltage characteristic and the rapid response of the junction without using the external shunt.

8. CONCLUSIONS

Thus, Josephson junctions with an internal shunt (and, first and foremost, junctions with doped amorphous silicon in the weak-coupling region) can have a size below 1 ± 1 μm^2 and provide (rather great against the background of thermal fluctuations) critical current $I_C \geq 100$ μA in this case, which opens the path to creating promising large-scale integration superconducting circuits on their basis.

Magnetic junctions with an internal shunt (and, first and foremost, junctions with magnetic doping of amorphous silicon), which provide the shifting of the Josephson phase by π in a state of stable equilibrium, provide a sharp decrease in the geometric inductance and, therefore, in the size of master logical cells for rapid single flux quantum logic.

Magnetic Josephson junctions with a weak ferromagnetic in the weak-coupling region can be used as Josephson memory elements with the size of such a memory element being determined by the size of just one junction. However, the characteristic frequency of such elements is rather small.

The generalization and evaluation of the results of the theoretical and experimental analysis of features of the current transport through magnetic Josephson structures with an auxiliary superconducting *s*-island in the weak-coupling region allow us to formulate the basic recommendations for the creation of

(1) A rapid memory element based on the SIsFS structure;

(2) A 0-π switch with a high characteristic frequency based on the SIsFS structure;

(3) A high-frequency memory element based on the Josephson heterostructure with two magnetic layers for implementation of a half-selective mechanism.

ACKNOWLEDGMENTS

This work was supported by the Ministry of Education and Science of the Russian Federation, the Dynasty Foundation, the President Grant (MK-1841.2014.2), and the Russian Foundation for Basic Research (project nos. 14-02-31002-mol-a and 14-02-90018-bel-a).

REFERENCES

1. S. Nishijima, S. Eckroad, A. Marian, et al., Supercond. Sci. Technol. **26**, 113001 (2013); O. A. Mukhanov, IEEE Trans. Appl. Supercond. **21**, 760 (2011).
2. D. S. Holmes, A. L. Ripple, and M. A. Manheimer, IEEE Trans. Appl. Supercond. **23**, 1701610 (2013).
3. R. Landauer, IBM J. Res. Dev. **3**, 183 (1961).
4. O. Mukhanov, D. Cupta, A. Kadin, and V. Semenov, Proc. IEEE **92**, 564 (2004).
5. J. Ren, V. K. Semenov, Y. A. Polyakov,D. V. Averin, and J. S. Tsai, IEEE Trans. Appl. Supercond. **19**, 961 (2009).
6. J. Ren and V. K. Semenov, IEEE Trans. Appl. Supercond. **21**, 780 (2011).
7. C. Bennett, IBM J. Res. Dev. **17**, 525 (1973).
8. Z. H. Gan, W. Q. Dong, L. M. Qiu, X. B. Zhang, H. Sun, Y. L. He, and R. Radebaugh, Cryogenics **49**, 198 (2009).
9. M. Y. Xu, A. T. A. M. de Waele, and Y. L. Ju, Cryogenics **39**, 865 (1999).

10. C. Wang, G. Thummes, and C. Heiden, Adv. Cryog. Eng. **43**, 2055 (1998).
11. W. C. Stewart, Appl. Phys. Lett. **12**, 277 (1968).
12. K. K. Likharev, Rev. Mod. Phys. **51**, 101 (1979).
13. http://www.hypres.com
14. M. Yu. Kupriyanov, A. Brinkman, A. A. Golubov, M.Yu. Kupriyanov, A. Brinkman, A.A. Golubov, M. Siegel, and H. Rogalla, Physica C, Supercond. Its Appl. **326–327**, 16 (1999).
15. M. Hidaka, S. Hagasawa, K. Hinode, and T. Satoh, IEICE Trans. Electron. **E91-C**, 318 (2008).
16. S. K. Tolpygo, D. Yohannes, R. T. Hunt, J. A. Vivalda, D. Donnelly, D. Amparo, and A. F. Kirichenko, IEEE Trans. Appl. Supercond. **17**, 946 (2007).
17. S. P. Benz, C. A. Hamilton, C. J. Burroughs, T. E. Harvey, and L. A. Christian, Appl. Phys. Lett. **71**, 1866 (1997).
18. A. Shoji and H. Yamamori, M. Ishizaki, S. P. Benz, and P. D. Dresselhaus, IEEE Trans. Appl. Supercond. **13**, 919 (2003).
19. A. L. Gudkov, M. Yu. Kupriyanov, and K. K. Likharev, Zh. Eksp. Teor. Fiz. **94**, 319 (1988).
20. A. L. Gudkov, M. Yu. Kupriyanov, and A. N. Samus', J. Exp. Theor. Phys. **114**, 818 (2012).
21. D. Olaya, B. Baek, P. Dresselhaus, and S. P. Benz, IEEE Trans. Appl. Supercond. **18**, 1797 (2008).
22. D. Olaya, P. Dresselhaus, S. P. Benz, J. Bjarnason, and E. N. Grossman, IEEE Trans. Appl. Supercond. **19**, 144 (2009).
23. D. Olaya, P. Dresselhaus, B. Baek, S. P. Benz, A. Herr, Q. P. Herr, A. G. Ioannidis, D. L. Miller, and A. W. Kleinsasser, Appl. Phys. Lett. **96**, 213510 (2010).
24. A. L. Gudkov, A. I. Kozlov, A. N. Samus', and I. Ya. Krasnopolin, *Proc. 5th All-Russ. Sci.-Tech. Conf. "Problems of Development of Perspective Micro- and Nanoelectron Systems"*, 2012.
25. K. K. Likharev, V. P. Koshelets, V. V. Migulin, O. A. Mukhanov, G. A. Ovsyannikov, V. K. Semenov, I. L. Serpuchenko, and A. N. Vystavkin, IEEE Trans. Magn. **23**, 755 (1987).
26. K. K. Likharev, V. K. Semenov, and O. A. Mukhanov, IEEE Trans. Magn. **23**, 759 (1987).
27. K. K. Likharev and V. K. Semenov, IEEE Trans. Appl. Supercond. **1**, 3 (1991).
28. W. Chen, A. V. Rylyakov, V. Patel, J. E. Lukens, and K. K. Likharev, IEEE Trans. Appl. Supercond. **9**, 3212 (1999).
29. T. Filippov, M. Dorojevets, A. Sahu, A. Kirichenko, C. Ayala, and O. Mukhanov, IEEE Trans. Appl. Supercond. **21**, 847 (2011).
30. S. Nagasawa, H. Numata, Y. Hashimoto, and S. Tahara, IEEE Trans. Appl. Supercond. **9**, 3708 (1999).
31. Q. Liu, K. Fujiwara, X. Meng, S. R. Whiteley, T. van Duzer, N. Yoshikawa, Y. Thakahashi, T. Hikida, and N. Kawai, IEEE Trans. Appl. Supercond. **17**, 526 (2007).
32. O. A. Mukhanov, A. F. Kirichenko, T. V. Filipov, and S. Sarwana, IEEE Trans. Appl. Supercond. **21**, 797 (2011).
33. L. N. Bulaevskii, V. V. Kuzii, and A. A. Sobyanin, J. Exp. Theor. Phys. Lett. **25**, 290 (1977).
34. A. I. Buzdin, L. N. Bulaevskij, and S. V. Panyukov, J. Exp. Theor. Phys. Lett. **34**, 178 (1982).
35. A. V. Ustinov and V. K. Kaplunenko, J. Appl. Phys. **94**, 5405 (2003).
36. T. Ortlepp, T. Ariando, O. Mielke, C. J. M. Verwijs, K. F. K. Foo, H. Rogalla, F. H. Uhlmann, and H. Hilgenkamp, Science **312**, 1495 (2006).
37. A. K. Feofanov, V. A. Oboznov, V. V. Bol'ginov, J. Lisenfeld, S. Poletto, V. V. Ryazanov, A. N. Rossolenko, M. Khabipov, D. Balashov, A. B. Zorin, P. N. Dmitriev, V. P. Koshelets, and A. V. Ustinov, Nature Phys. **6**, 593 (2010).
38. A. M. Kadin, C. A. Mancini, M. J. Feldman, and D. K. Brock, IEEE Trans. Appl. Supercond. **11**, 1050 (2001).
39. N. G. Pugach, E. Goldobin, R. Kleiner, and D. Koelle, Phys. Rev. B: Condens. Matter Mater. Phys. **81**, 104513 (2010).
40. E. Goldobin, H. Sickinger, M. Weides, N. Ruppelt, H. Kohlstedt, R. Kleiner, and D. Koelle, Appl. Phys. Lett. **102**, 242602 (2013). http://dx.doi.org/10.1063/1.4811752
41. S. V. Bakurskiy, N. V. Klenov, T. Yu. Karminskaya, M. Yu. Kupriyanov, and A. A. Golubov, Supercond. Sci. Technol. **26**, 015005 (2013).
42. H. Haken, *Quantum Field Theory of Solids* (Elsevier, 1976; Moscow, 1980).
43. A. Zagoskin, *Quantum Theory of Many-Body Systems: Techniques and Applications* (New-York, 1998).
44. A. I. Buzdin and M. Yu. Kupriyanov, Pism. Zh. Eksp. Teor. Fiz. **53**, 321 (1991).
45. V. V. Ryazanov, Phys.-Usp. **42**, 825 (1999).
46. S. Oh, D. Youm, and M. Beasley, Appl. Phys. Lett. **71**, 2376 (1997).
47. D. Youm and M. Beasley, US Patent 6233171 B1, 2001.
48. Johnson et al., US Patent 6414870 B1, 2002.
49. R. Held, J. Xu, A. Schmehl, C. W. Schneider, J. Mannhart, and M. R. Beasley, Appl. Phys. Lett. **89**, 163509 (2006).
50. T. Yu. Karminskaya, A. A. Golubov, M. Yu. Kupriyanov, and A. S. Sidorenko, Phys. Rev. B: Condens. Matter Mater. Phys. **79**, 214509 (2009).
51. T. Yu. Karminskaya, A. A. Golubov, M. Yu. Kupriyanov, and A. S. Sidorenko, Phys. Rev. B: Condens. Matter Mater. Phys. **81**, 214518 (2010).
52. F. S. Bergeret, A. F. Volkov, and K. B. Efetov, Phys. Rev. Lett. **86**, 3140 (2001).
53. A. A. Golubov, M. Yu. Kupriyanov, and Ya. V. Fominov, JETP Lett. **75**, 190 (2002).
54. V. V. Bol'ginov, V. S. Stolyarov, D. S. Sobanin, A. L. Karpovich, and V. V. Ryazanov, JETP Lett. **95**, 366 (2012).
55. L. S. Uspenskaya, A. L. Rakhmanov, L. A. Dorosinskiy, V. S. Stolyarov, O. V. Skryabina, S. V. Egorov, and A. A. Chugunov, JETP Lett. **97**, 155 (2013).
56. M. Eschrig, Phys. Today **64**, 43 (2011).
57. J. W. A. Robinson, J. D. S. Witt, and M. G. Blamire, Science **329**, 59 (2010).

58. C. Klose, T. S. Khaire, Y. Wang., W. P. Pratt, N. O. Birge, B. J. McMorran, T. P. Ginley, J. A. Borchers, B. J. Kirby, B. B. Maranville, and J. Unguris, Phys. Rev. Lett. **108**, 127002 (2012).
59. A. Y. Herr and Q. P. Herr, US Patent 8 270 209 B2, 2010.
60. S. V. Bakurskiy, N. V. Klenov, I. I. Soloviev, V. V. Bol'ginov, V. V. Ryazanov, I. V. Vernik, O. A. Mukhanov, M. Yu. Kupriyanov, and A. A. Golubov, Appl. Phys. Lett. **102**, 192603 (2013). http://dx.doi.org/10.1063/1.4805032
61. S. V. Bakurskiy, N. V. Klenov, I. I. Soloviev, M. Yu. Kupriyanov, and A. A. Golubov, Phys. Rev. B: Condens. Matter Mater. Phys. **88**, 144519 (2013).
62. M. I. Khabipov, D. V. Balashov, F. Maibaum, A. B. Zorin, V. A. Oboznov, V. V. Bolginov, A. N. Rossolenko, and V. V. Ryazanov, Supercond. Sci. Technol. **23**, 045032 (2010).
63. N. V. Klenov, N. G. Pugach, A. V. Sharafiev, S. V. Bakurskiy, and V. K. Kornev, Phys. Solid State **52**, 2246 (2010).
64. M. Yu. Kupriyanov, S. V. Bakurskii, N. V. Klenov, and I. I. Solov'ev, RF Patent No. 2013144619 (2013).
65. N. V. Klenov, A. V. Sharafiev, S. V. Bakurskiy, and V. K. Kornev, IEEE Trans. Appl. Supercon. **21**, 864 (2011).
66. T. S. Rumyantseva, N. G. Pugach, and N. V. Klenov, Mos. Univ. Phys. Bull. **66**, 28 (2011).
67. M. Yu. Kupriyanov, S. V. Bakurskii, N. V. Klenov, I. I. Solovyev, A. L. Gudkov, and V. V. Ryazanov RF Patent 2013127417, 2013.
68. S. Baburin and A. Samodelov, Komp. Tekhnol. **10**, 51 (2012). http://www.everspin.com

Translated by Yu. Kornienko